Research in Astron. Astrophys. **2013** Vol. **13** No. **12**, 1482–1492
http://www.raa-journal.org *http://www.iop.org/journals/raa*

Research in Astronomy and Astrophysics

The breakdown of the power-law frequency distributions for the hard X-ray peak count rates of solar flares *

You-Ping Li[1], Wei-Qun Gan[1], Li Feng[1], Si-Ming Liu[1] and A. Struminsky[2]

[1] Key Laboratory of Dark Matter and Space Astronomy, Purple Mountain Observatory, Chinese Academy of Sciences, Nanjing 210008, China; *yplee@pmo.ac.cn*

[2] Space Research Institute (IKI), Russian Academy of Science, Profsoyuznaya Str. 84/32, 117997, Moscow, Russia

Received 2013 May 29; accepted 2013 June 23

Abstract The frequency distribution for several characteristics of a solar flare obeys a power law only above a certain threshold, below which there is an apparent loss of small scale events presumably caused by limited instrumental sensitivity and the corresponding event selection bias. It is also possible that this deviation in the power law can have a physical origin in the source. We propose two fitting models incorporating a power law distribution with a low count rate cutoff plus a noise component for the frequency distribution of the hard X-ray peak count rate of all solar flare samples obtained with HXRBS/SMM and BATSE/CGRO observations. Our new fitting method produces the same power-law index as previously developed methods, a low cutoff of the power-law function and its corresponding noise level, which is consistent with measurements of the actual noise level of the hard X-ray count rate. We found that the fitted low cutoff appears to be related to the noise level, i.e., flares are only recognized when their peak count rate is 3σ greater than noise. Therefore, the fitted low cutoff, which is smaller than the aforementioned threshold, might be attributed to selection bias, and probably not to the actual count rate cutoff in flares at smaller scales. Whether or not the actual low cutoff physically exists needs to be checked by future observations with increased sensitivities.

Key words: Sun: flares — Sun: X-rays, gamma-rays — methods: statistical

1 INTRODUCTION

Power-law distributions commonly exist in various phenomena related to nature and human life (Newman 2005), for instance, the distribution describing magnitudes of earthquakes (Gutenberg & Richter 1954); the distribution of the number of creatures comprising different species (Willis & Yule 1922); the distribution of file sizes saved in computers (Crovella & Bestavros 1997); the distribution of intensities of wars (Roberts & Turcotte 1998); the distribution of the times that a word in a human language is used (Zipf 1949); the distribution of the number of papers written by scientists (Lotka 1926); the distribution of the number of paper citations (de Solla Price 1965), etc. In solar physics, power-law distributions in different phenomena have been broadly investigated, e.g., by Aschwanden

* Supported by the National Natural Science Foundation of China.

(2011) and references therein, and recently by Li et al. (2012), Song et al. (2012), Aschwanden (2012) and Aschwanden & Freeland (2012). A power-law frequency distribution indicates that the number of events (frequency) is a power-law function of the scale of these events

$$\mathrm{d}N = A\,x^{-\delta}\mathrm{d}x, \tag{1}$$

where $\mathrm{d}N$ denotes the number of events recorded in the interval $[x, x + dx]$ (x describes, e.g., the hard X-ray (HXR) peak count rate of flares), and δ and A are constants which can be determined from a fit to data.

Usually, a power-law distribution can only be satisfied above a certain threshold x_b, below which the number of events is less than what is expected from the downward extrapolation of the power-law distribution. The distribution curve shows an apparent loss of small-scale events. In general, the deviation from a power law is due to the limited sensitivity of an instrument and the related flare selection bias. The low count rate threshold for the power-law distribution of flares derived from observations with the Hard X-Ray Burst Spectrometer (HXRBS) (Orwig et al. 1980) on the Solar Maximum Mission (SMM) with a detector area of 71 cm^2 is different by about one order of magnitude from that derived from measurements with the Burst and Transient Source Experiment (BATSE) (Fishman et al. 1992) on the Compton Gamma-Ray Observatory (CGRO), whose detector area is 2025 cm^2. On the other hand, an intrinsic low cutoff is necessary to ensure the convergence of a distribution with $\delta > 1$. In soft X-ray (SXR), the background flux of flares depends on the level of solar activity. The low threshold x_b of a power-law distribution of peak flux/count rate also depends on solar activity (e.g., Veronig et al. 2002). The variation of x_b with solar activity in power-law fittings to SXR peak flux is not caused by instrument sensitivity, as it is invariant through different levels of solar activity, but rather is caused by fluctuations in the flux of the flare background in SXR which depends on solar activity. Feldman et al. (1997) compiled statistics on the SXR flares at different levels of background flux, and found that the power-law distribution could be extended to A2.0 class flares, and the power-law index was consistent with the one derived from the samples of flares that belong to higher classes. If the flux of an SXR flare is scaled to its corresponding background, the frequency distribution for all samples of flares can be approximated by a single power law without any deviation at low fluxes (Gan et al. 2012).

Figure 1 illustrates the deficiency of events at small scales by two examples adopted from Crosby et al. (1993). The top panel is the frequency distribution of the HXR peak count rate of flares observed by SMM from 1980 to 1982. The fitted power-law function is indicated by a thick gray line. Downwards from the count rate around 30 count s^{-1}, the frequency drops dramatically by almost two orders of magnitude. The bottom panel presents the frequency distribution of the energy carried by electrons obtained from spectral fits to HXR for the selected events which have peak counts larger than 100 count s^{-1}. At about 10^{28} erg, the distribution starts to show the deviation from a power law. It stays nearly constant for energies lower than 10^{28} erg. These two examples reveal two representative deficiencies for small-scale events. One category shows a significant decrease in the number of events at smaller scales below the threshold x_b, but the frequency of small-scale events stays almost constant in the other category. Another prominent difference between these two categories is the range of count rate or energy below the threshold x_b. It appears that the second category spans over three orders of magnitude from 10^{25} to 10^{28} erg. However, the range in count rate below x_b in the first category is much narrower, which is from 1 to 30 count s^{-1}. One should also note that the first example is obtained directly from the observed data, but the second example gives the distribution for the total energy of electrons above 25 keV, which is derived from the observed count spectrum based on an emission model.

In this paper, we will investigate how and why the frequency distributions of peak count rate for flares have such a deviation at its lower end. In Section 2, our new fitting model is described. In Section 3, we apply this new model to observations made by HXRBS/SMM and BATSE/CGRO. The discussions and conclusions are included in the last section.

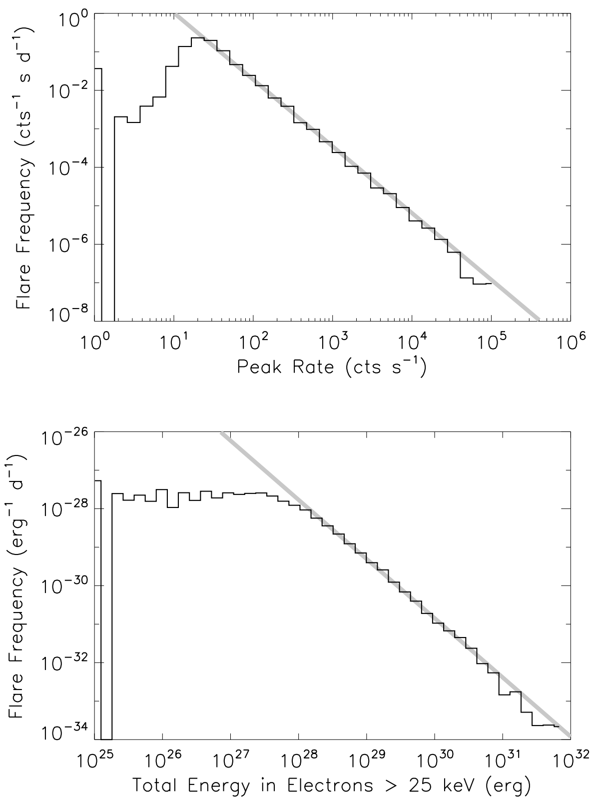

Fig. 1 Two examples of power-law frequency distributions showing the deficiency of events at small scales. (*Top*) The frequency distribution of the peak count rate for 7045 HXRBS flares during 1980–1982. (*Bottom*) The frequency distribution of the total energy carried by electrons above 25 keV during the duration of the flare. The thick lines display the fitted power-law functions. All the data are adopted from Crosby et al. (1993).

2 NEW FITTING MODEL

Considering a power-law function defined by Equation (1), if we shift x by a small amount δx, the resulting function will deviate from the power law and follow the form $g(x) \propto (x + \delta x)^{-\delta}$. In this section, we will investigate two different models of δx, the term which actually represents the noise or which can be understood as the inherent measurement error, to understand how they will change the original power-law frequency distribution.

If we assume white noise for the measurement error, its probability density function (PDF) is a uniform distribution. We set its two boundaries at $-x_n$ and x_n. In other words, the maximum of the noise level is x_n. Explicitly, the PDF can be formulated as

$$n(z) = \begin{cases} \frac{1}{2x_n}\,, & -x_n < z < x_n\,, \\ 0\,, & \text{otherwise}\,. \end{cases} \tag{2}$$

Another more popular form of noise has a Gaussian distribution as its PDF

$$n(z) = \frac{1}{\sqrt{2\pi}\sigma} \mathrm{e}^{-\frac{z^2}{2\sigma^2}}\,. \tag{3}$$

The uniform distribution is an approximation of the Gaussian distribution when the standard deviation σ is large enough.

We assume the true distribution of a given sample in variable y follows a power law with a low cutoff x_c

$$p(y) = \begin{cases} \frac{\delta-1}{x_c^{\delta-1}} y^{-\delta}\,, & y \geqslant x_c\,, \\ 0\,, & y < x_c\,, \end{cases} \tag{4}$$

where δ is the power-law index. Supposing the true value y and its noise z are independent variables, then the PDF of the measurements $x = y + z$ can be written as

$$f(x) = \int_{-\infty}^{+\infty} n(z)p(x-z)dz = \int_{-\infty}^{+\infty} p(y)n(x-y)dy\,. \tag{5}$$

Substituting functions of $n(z)$ and $p(y)$ by Equations (2) and (4), and after some reduction steps, we arrive at

$$f(x) = \begin{cases} \frac{1}{2x_n x_c^{1-\delta}}[(x-x_n)^{1-\delta} - (x+x_n)^{1-\delta}]\,, & x > x_n + x_c\,, \\ \frac{1}{2x_n x_c^{1-\delta}}[x_c^{1-\delta} - (x+x_n)^{1-\delta}]\,, & x \leqslant x_n + x_c\,. \end{cases} \tag{6}$$

In the case of Gaussian noise, $f(x)$ is calculated as

$$f(x) = \frac{\delta-1}{x_c^{\delta-1}\sqrt{2\pi}\sigma} \int_{x_c}^{+\infty} y^{-\delta} \mathrm{e}^{-\frac{(x-y)^2}{2\sigma^2}}\, dy\,. \tag{7}$$

Unfortunately, the integration cannot be obtained analytically as in Equation (7). The integration in Equation (7) is analogous to the one in the thin-target model, replacing the cross section of the electron-ion bremsstrahlung by a Gaussian function. Since the computation of the integration is usually time-consuming, a fast algorithm (Li & Gan 2011) was adopted based on the method by Holman and Su (*http://hesperia.gsfc.nasa.gov/ssw/packages/xray/doc/brm_thick_doc.pdf*). We find that when $x \gg x_n + x_c$ (or $\sigma + x_c$), Equations (6) and (7) can be approximated by a power law, whereas they deviate from a power law when $x \lesssim x_n + x_c$ (or $\sigma + x_c$).

Figure 2 displays some plots that investigate parameterizations of Equations (6) and (7). We fixed the value of the power-law index $\delta = 1.7$. For the uniformly distributed noise, x_n is set to 300. For the Gaussian noise, σ is set to 200. What we varied is the low cutoff of the power-law distribution x_c. In Figure 2(a), $x_c = 1$. Two PDF functions follow the power law for $x \gtrsim 1000$ with their indices δ still equal to 1.7. When $x \lesssim 300$, they deviate from the power law and stay constant. In the interval between 50 to 500, the two PDF functions become elevated to a level above the pure power-law function. x_c is increased to 100 in Figure 2(b). The PDF functions deviate at $x \approx 400$ and stay almost constant in the downwards direction but with a very slight decrease. The shape of functions defined by Equations (6) and (7) resembles the frequency distribution of flare energy in the bottom panel of Figure 1. When x_c reaches the noise level x_n, these functions start to deviate from $x \approx 600$ and show a descending trend towards $x = 0$. In Figure 2(d) and (e), the function defined by Equation (6) has a shape similar to the frequency distribution of the flare peak count rate in the upper panel of Figure 1. When x_c is much larger than the noise level x_n, the part of the power law that deviates from that function shows a very dramatic drop (Fig. 2(f)). With the increase of x_c, the range of x that deviates shrinks. In general, from Figure 2(a) to (f), the function defined by Equation (7) follows a similar trend as that defined by Equation (6) when x_c increases from 1 to 3000. The major difference is that in Figure 2(d) and (e) the function defined by Equation (7) has a longer tail below the cutoff x_c. In addition to the variation of $f(x)$ with the parameter x_c, we find that the low cutoff x_c defined in the power-law function in Equation (4) is always smaller than the low threshold above which $f(x)$ follows a power law.

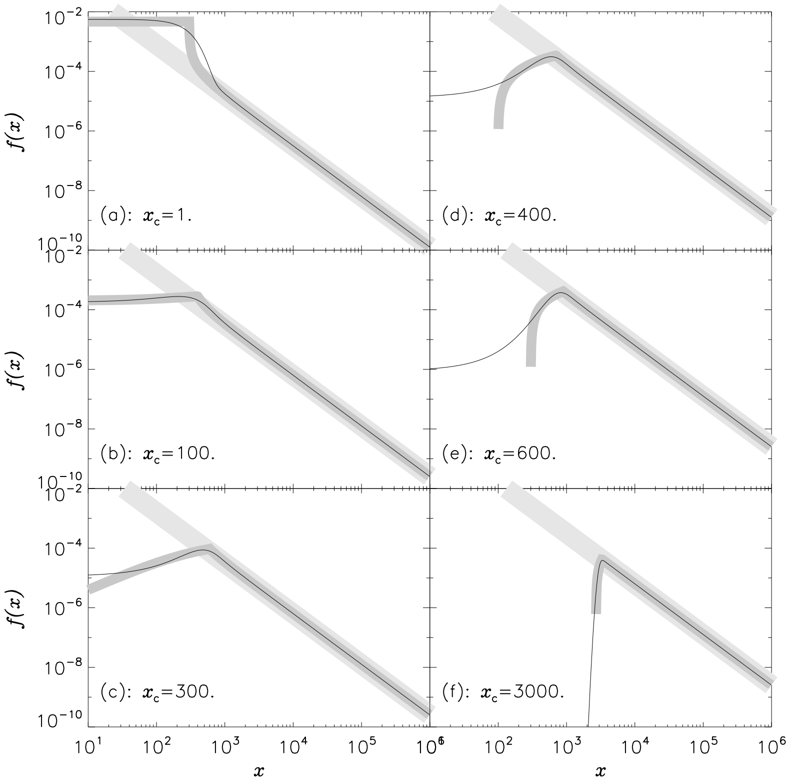

Fig. 2 Fitting functions for different values of low cutoff x_c. The power-law index $\delta = 1.7$. For the white noise, x_n is set to 300. For the Gaussian noise, σ is set to 200. From (a) to (f), x_c varies from 1 to 3000. The thickest line is a pure power-law function, the lines with intermediate thickness represent the fitting functions that combine the power law and the white noise (Eq. (6)), and the thinnest lines account for the fitting functions that combine the power law and the Gaussian noise (Eq. (7)).

3 MEASUREMENTS AND FITTINGS

Two existing methods are often applied to the power-law fitting of a frequency distribution. Method 1 (e.g., Veronig et al. 2002) firstly divides the measurements in the logarithm space by equal-width bins to derive their differential frequency distribution. Then a linear fit is applied to such a differential distribution in the log-log scale. Method 2 is the maximum likelihood method applied directly to measurements to derive a power-law index, e.g., Crosby et al. (1993) and Clauset et al. (2009). Both methods have to determine a reasonably low threshold x_b for the fitting. If x_b is too low, the derived power-law index tends to be underestimated. If x_b is too high, we lose the information about some useful samples. Clauset et al. (2009) applied the Kolmogorov-Smirnov (KS) statistic (Press et al. 1992) to determine x_b. The derived x_b can be used in method 1 as well.

The peak count rate of 7045 flares recorded by HXRBS/SMM during 1980 to 1982 is used as the first data set in this paper. Crosby et al. (1993) set the low threshold x_b to 30 count s^{-1} and made a power-law fit to it with method 2, and obtained an index of 1.732. More flare samples observed by HXRBS in 1980–1982 were analyzed by Dennis (1985) and a similar power-law index of about 1.8

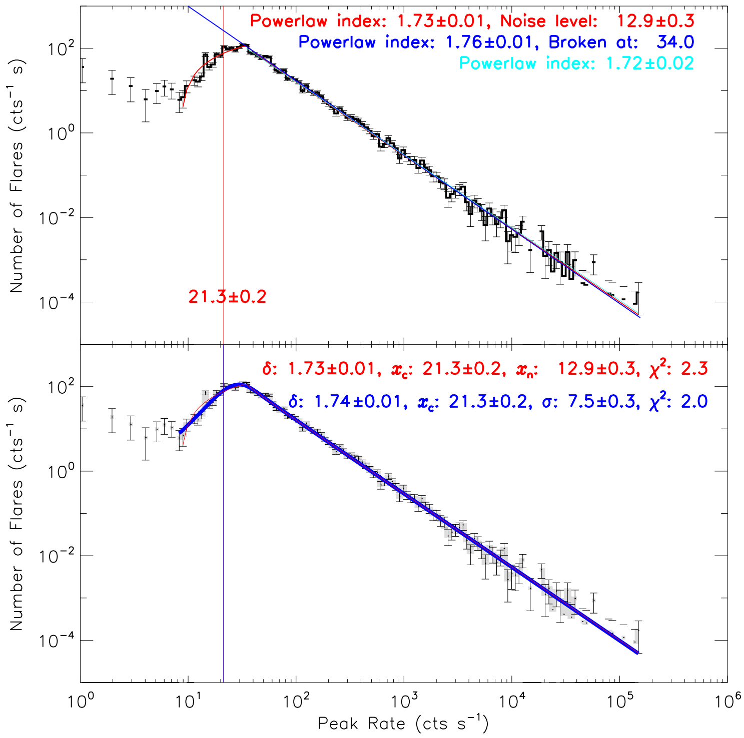

Fig. 3 The frequency distribution of the flare peak flux recorded by HXRBS/SMM in 1980-1982. The error bars represent $\pm 1\sigma$ uncertainties based on the Poisson statistics for the number of flares in each bin. An averaged background of 40 count s^{-1} was subtracted from the peak rate listed in the HXRBS catalog (*http://umbra.gsfc.nasa.gov/smm/hxrbs/*). (*Top*) The cyan line and text display the linear fit of a power-law function in the log-log space (method 1), the blue line and text represent the fitting result with the maximum likelihood method (method 2), and the red line and text indicate our nonlinear fit using the function defined by Equation (6) (method 3). The red vertical line and the number mark the low cutoff x_c in the function defined by Equation (6). (*Bottom*) Comparison of the fitting results using the function defined by Equation (6) in red and that defined by Equation (7) in blue.

was derived. A complete data set for HXRBS flares during 1980–1989 was statistically investigated by Schwartz et al. (1992). The authors found a power-law index of 1.73.

The functions defined by Equations (6) and (7) have been normalized. For the purpose of a fitting to the observed frequency distributions, we introduce an additional parameter a which denotes the peak of frequencies for functions defined by Equations (6) and (7). A total of four free parameters will be fitted to the frequency distributions derived from observations. For the function defined by Equation (6), they are the peak frequency, a, the noise level x_n, the power-law low cutoff x_c and index δ. For the function defined by Equation (7), three parameters are the same as those for the function defined by Equation (6). What differs is that x_n is replaced with σ. The four parameters will be determined by nonlinear fittings to the frequency distributions.

Figure 3 illustrates the fittings to the frequency distribution of the HXR peak count rate of 7045 flares recorded by HXRBS/SMM with three different methods. As in Crosby et al. (1993), the background of an averaged count rate over the whole data set of 40 count s^{-1} was subtracted. The frequency distribution in the log space was equally divided into 150 bins (about 32 bins in Crosby

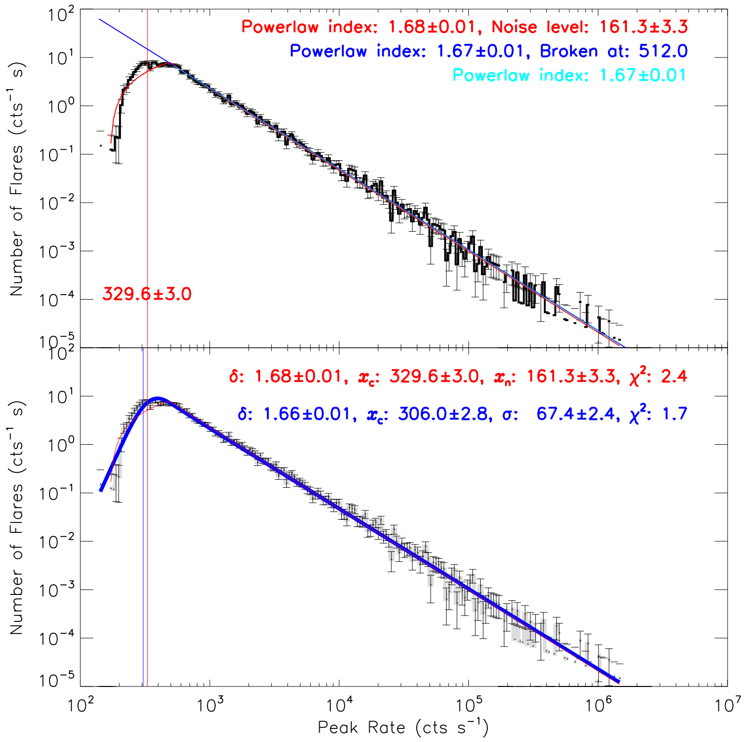

Fig. 4 Frequency distribution of the peak count rate of the flares in the 25–100 keV energy band recorded by BATSE in 1991–2000. The error bars represent $\pm 1\sigma$ uncertainties based on Poisson statistics on the number of flares in each bin. An average background was subtracted from the peak rate for each flare. The lines and texts share the same color code as in Fig. 3.

et al. 1993). The error bars are $\pm 1\sigma$ uncertainties based on the Poisson statistics for the number of flares in each bin. In the upper panel of Figure 3, the blue line derived from method 2 shows a power-law function with an index of 1.76 ± 0.01 and a low threshold x_b of 34 count s^{-1} by the KS method (Press et al. 1992). Taking the same value of x_b, the linear fit (method 1) yields an index of 1.72 ± 0.02. The red line displays the fitting using our function defined by Equation (6) (method 3). The derived parameters are $\delta = 1.73 \pm 0.01$, $x_c = 21.3 \pm 0.2$ count s^{-1} and $x_n = 12.9 \pm 0.3$ count s^{-1}. The power-law index derived from method 3 lies between the indices resulting from methods 1 and 2. Note that the subtracted background was averaged over the whole data set, and is not the background for individual flares. It caused some unreasonable negative count rates for a subset of flares. Therefore, we did not take the whole data set of the 7045 flares and only consider the flare samples whose peak rate is greater than 8 count s^{-1}. In the bottom panel of Figure 3, the comparison between the results from fitting the functions defined by Equations (6) in red and (7) in blue is presented. They produce similar power-law indices and low cutoffs. Parameters related to noise represent different meanings in the two functions, and therefore have different values. From the value of χ^2, it appears that the function defined by Equation (7) better fits the frequency distribution.

In Figure 4, the frequency distribution of the peak rate of HXR flares in the 25–100 keV energy band recorded by BATSE is presented. Subsets of these flare samples have been analyzed by a couple of authors. The derived power-law indices of 1.61 ± 0.03 were published by Schwartz et al. (1992), and 1.75 ± 0.02 by Biesecker et al. (1994). From 1991 to 2000, BATSE observed a total of 7372 flare samples (*ftp://umbra.nascom.nasa.gov/pub/batse/*). Because BATSE had a large detector area of 2025 cm^2, the peak rate of some flares was saturated. We excluded those saturated ones whose peak counts are beyond $3{\times}10^6$ count s^{-1} and in the end collected 7365 samples. The following analyses are focused on this subset of flares.

With the range of peak flux equally divided into 210 bins, as in Figure 3, we adopted three different methods to make the fittings. For methods 1 and 2, the low threshold x_b was again determined with the maximum likelihood method. Only the part above x_b could be fitted by a power law. Method 3 allows us to fit to the whole range associated with the peak rate. Method 2 produces a power-law index of 1.67 ± 0.01 and a low threshold x_b of 512 count s^{-1}. Taking the same x_b, method 1 has a similar index as method 2. Method 3 performs a nonlinear fitting of the function defined by Equation (6) to the data points in all 210 bins. We found that $\delta = 1.68 \pm 0.01$, $x_n = 161.3 \pm 3.3$ count s^{-1} and $x_c = 329.6 \pm 3.0$ count s^{-1}. A comparison of the results using functions defined by Equations (6) and (7) is presented in the bottom panel. There is only a small difference between them, but the fitting using the function defined by Equation (7) is slightly better.

4 DISCUSSION AND CONCLUSIONS

We have developed a new fitting model for the frequency distributions of flare parameters, in which we found that the random noise inherent in measurements can cause a deviation from the power-law function close to its lower end. With the newly constructed fitting functions, we made fittings to the frequency distributions of the HXR peak count rate of solar flares recorded by HXRBS/SMM in 1980–1982 and BATSE/CGRO in 1991–2000. Compared with previously existing methods, our new fitting functions can be fitted to the frequency distributions over the whole peak flux range, but the previous methods have to set a low threshold above which the distribution is fitted by a power law. Actually, we find that the peak rate of all flare samples obeys a power law, and the apparent deficiency of frequency in the lower end could be caused by the noise.

In addition to the power-law index, new fitting functions allow us to derive the low cutoff of a power-law distribution x_c (which is smaller than the apparent low threshold x_b) and the noise level. The noise level is instrument dependent and refers to fluctuations in the instrument's output when there is no input signal. We have checked whether the derived noise level from the fittings is consistent with the specific observed value or not. The top two panels of Figure 5 show the light curves of two flare events observed in HXR by BATSE after the background was subtracted. One event is the first flare in the BATSE catalog, and the other one is close to the end of the BATSE mission. To enhance the fluctuations from noise, a high-pass filter was applied. The resulting evolution is indicated by the thin solid lines. We found that for these two events, the observed noise level is consistent with the one obtained from fitting the frequency distributions in which the noise level was $x_n = 161.3$ count s^{-1}. The bottom two panels are the light curves and fluctuations from noise in two flare samples recorded by HXRBS. (S1) illustrates the results of the first flare in the HXRBS catalog, and (S2) is a representative example chosen by Dennis et al. (1991) to demonstrate the definition of each item in the HXRBS flare catalog. For these two flare examples, we found that the observed noise level is also comparable to the value derived from the fitting. Therefore, we conclude that the noise level inferred from the fittings of frequency distributions actually reflects the true fluctuations from noise in the data. Note that the fluctuations from noise we are discussing here do not take into account the remaining signal from subtracting the background of the flare. The backgrounds of some flares were over-subtracted, but there are also some flares which were under-subtracted. Therefore, some remaining background signal could enter the peak count rate of the flare, and it produces another source of data fluctuation which differs from the sensitivity of the instrument. More precisely, in addition to the instrumental effect, the fitted noise level also has a contribution from the remaining background signal which might be greater than the instrumental fluctuation, especially when the count rate is small and the background is high.

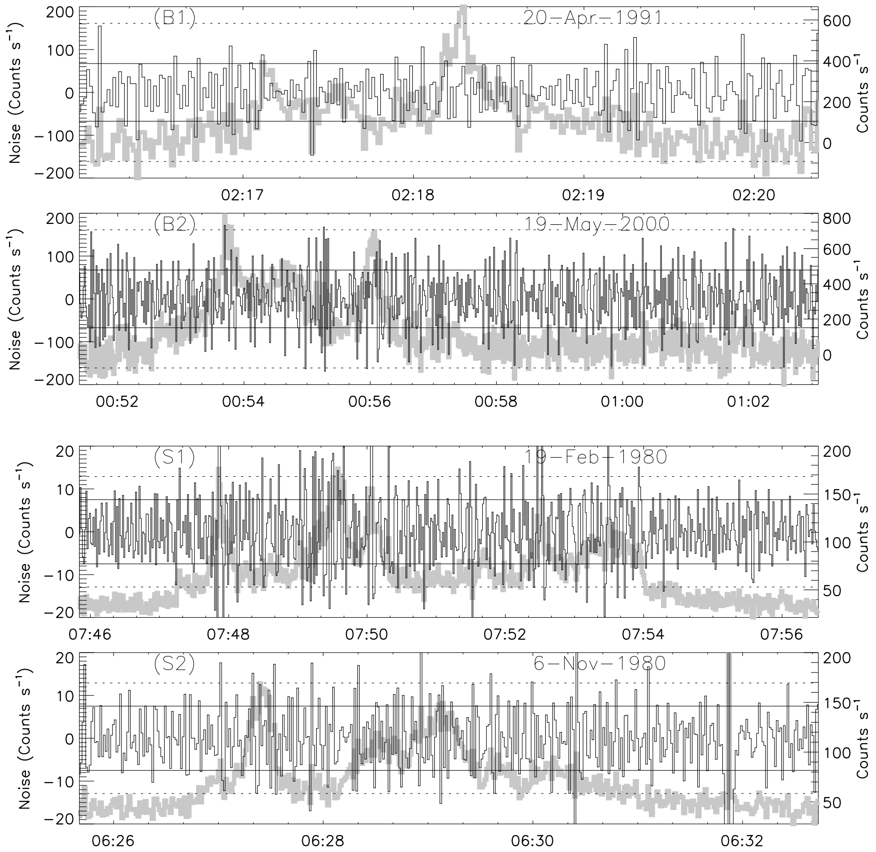

Fig. 5 The light curves and fluctuations from noise of two flare events selected from the BATSE (background subtracted) and HXRBS/SMM flare catalogs respectively. (B1) The light curve in the 25–50 keV energy band of the first flare recorded by BATSE is represented by the thick gray line. The low frequency components in the light curve were filtered out to make the fluctuations from noise more pronounced (*thin solid line*). The dotted horizontal line marks the noise level $x_n = 161.3$ count s^{-1} in the function defined by Equation (6), and the solid horizontal line accounts for the standard deviation $\sigma = 67.3$ count s^{-1} in the function defined by Equation (7). (B2) Same as (B1) but for a flare sample close to the end of the BATSE mission. (S1) The light curve in the 30–500 keV energy band of the first flare event in the HXRBS catalog (*thick gray line*) and its filtered high-pass components (*thin solid line*). Horizontal lines represent the noise levels of $x_n = 12$ count s^{-1} (*dotted lines*) and $\sigma = 7.5$ count s^{-1} (*solid lines*). (S2) Another flare sample in the HXRBS catalog was also used as an example in Dennis et al. (1991).

The low cutoff x_c of the power-law distributions can be interpreted in two ways: the sensitivity of an instrument, and a real cut-off of the measured flare parameter. For the discussions below, in Table 1 we listed the detector area $A_{\rm det}$ that is related to the instrument and the fitting results for the frequency distributions of the HXR peak flux with our new fitting functions. If x_c represents a real low cutoff of the measured count rate for the flare peak, that is to say, there is no flare sample that can reach the peak rate that is lower than x_c, then x_c scaled by the detector area should be the same. However, for HXRBS and BATSE, it turns out that the scaled x_c values are 0.30 and 0.16 count s^{-1} cm^{-2}, respectively, which are not consistent with each other. Note that our discussion

Table 1 The detector area of HXRBS and BATSE, and the fitted results for the frequency distributions of the HXR peak flux with our new fitting functions. The results from the function defined by Equation (7) are indicated in brackets.

Instrument	HXRBS	BATSE
$A_{\rm det}$ (cm^2)	71	2025
$x_n(\sigma)$ (count s^{-1})	$12.9 \pm 0.3(7.5 \pm 0.3)$	$161.3 \pm 3.3(67.3 \pm 2.4)$
x_c (count s^{-1})	$21.3 \pm 0.2(21.3 \pm 0.2)$	$329.6 \pm 3.0(306.0 \pm 2.8)$
x_b (count s^{-1})	34	512
δ	$1.73(1.74) \pm 0.1$	$1.68(1.66) \pm 0.1$

did not include the difference in the instrument response efficiency and the energy band in which the flare peak rate was measured (30–500 keV for HXRBS and 25–100 keV for BATSE). A firmer conclusion can be made when taking all these factors into account.

An alternative interpretation of the low cutoff x_c is from an instrumental point of view. This probably reflects its sensitivity. For the frequency distributions derived from HXRBS and BATSE, the obtained noise level x_n for both is around half of x_c. From the fittings that use the function defined by Equation (7), we are able to derive the standard deviation σ of the Gaussian noise. Supposing it is equivalent to the true fluctuations in the data, the inferred x_c is at the level of 2.8σ for HXRBS, and 4.5σ for BATSE, which are close to the 3σ threshold that is often used to determine a valid signal. Based on the discussions above, the low cutoff x_c is more probably caused by the sensitivity of the instruments, and is probably not due to the real physical low cutoff of the measured count rate for the flare peak. At least for HXRBS and BATSE, the real physical low cutoff, if it exists, should be below the sensitivity of their instruments.

Usually the selection bias has an influence on the frequency distributions, for instance, the deviation of a power law at its low end (Parnell & Jupp 2000; Aschwanden & Charbonneau 2002), and even the index of a power law (Aschwanden & Charbonneau 2002; Aschwanden & Parnell 2002). The frequency distribution of the HXR peak count rate investigated in this paper is also subject to the problem of bias. The downloaded flare list has been filtered according to some selection bias. Although it is not explicitly stated in the flare list, our fittings indicate that a flare was identified when the measurement was 3σ greater than fluctuations from noise.

When comparing the frequency distribution of flare energy in the bottom panel of Figure 1 with the fitting functions in Figure 2, we found that the frequency distribution of energy resembles Figure 2(b). The corresponding low cutoff x_c of the power-law distribution is smaller than the noise levels x_n and σ. Therefore, the relatively large noise makes the frequency distribution at low flare energies flat, and the power-law distribution of the flare energy can actually be extended to a value x_c that is lower than the apparent point that breaks down at x_b. This has been confirmed by quite a few studies on the frequency distributions of the flare energy (Crosby et al. 1993; Shimizu 1995; Aschwanden et al. 2000; Parnell & Jupp 2000; Benz & Krucker 2002; Hannah et al. 2008; Li et al. 2012).

Notice that the functions defined by Equations (6) and (7) are limited to the power-law functions with a single index, and cannot be applied to some more complicated distributions, e.g., frequency distributions of flare parameters should be fitted by a two-index broken power-law function (Su et al. 2006). This drawback can be overcome by making the simple power-law function more sophisticated and adopting other more complicated forms of noise. Then fitting functions other than those shown in Figure 2 can be constructed.

Acknowledgements This work is supported by the National Basic Research Program of China (973 Program, 2011CB811402), the National Natural Science Foundation of China (Grant

Nos. 11233008, 11078025, 11173063 and 11003047) and by Grant BK2012889. L. F. also acknowledges the Key Laboratory of Dark Matter and Space Astronomy, CAS, for financial support.

References

Aschwanden, M. J., Tarbell, T. D., Nightingale, R. W., et al. 2000, ApJ, 535, 1047

Aschwanden, M. J., & Charbonneau, P. 2002, ApJ, 566, L59

Aschwanden, M. J., & Parnell, C. E. 2002, ApJ, 572, 1048

Aschwanden, M. J. 2011, Self-Organized Criticality in Astrophysics (Berlin: Springer-Praxis)

Aschwanden, M. J. 2012, A&A, 539, A2

Aschwanden, M. J., & Freeland, S. L. 2012, ApJ, 754, 112

Benz, A. O., & Krucker, S. 2002, ApJ, 568, 413

Biesecker, D. A., Ryan, J. M., & Fishman, G. J. 1994, in Lecture Notes in Physics, Berlin Springer Verlag 432, Advances in Solar Physics, eds. G. Belvedere, M. Rodono, & G. M. Simnett, 225

Clauset, A., Shalizi, C. R., & Newman, M. E. J. 2009, SIAM Review, 51, 661

Crosby, N. B., Aschwanden, M. J., & Dennis, B. R. 1993, Sol. Phys., 143, 275

Crovella, M. E., & Bestavros, A. 1997, Networking, IEEE/ACM Transactions on, 5, 835

de Solla Price, D. J. 1965, Science, 149, 510

Dennis, B. R. 1985, Sol. Phys., 100, 465

Dennis, B. R., Orwig, L. E., Kennard, G. S., et al. 1991, The Complete Hard X-ray Burst Spectrometer Event List, 1980–1989, 4332 (National Aeronautics and Space Administration, Office of Management, Scientific and Technical Information Program)

Feldman, U., Doschek, G. A., & Klimchuk, J. A. 1997, ApJ, 474, 511

Fishman, G. J., Meegan, C. A., Wilson, R. B., Paciesas, W. S., & Pendleton, G. N. 1992, in NASA Conference Publication, 3137, eds. C. R. Shrader, N. Gehrels, & B. Dennis, 26

Gan, W. Q., Li, Y. P., & Feng, L. 2012, EAS Publications Series, 55, 239

Gutenberg, B., & Richter, C. F. 1954, Seismicity of the Earth and Associated Phenomena (2nd ed.; Princeton, NJ: Princeton Univ. Press), 310

Hannah, I. G., Christe, S., Krucker, S., et al. 2008, ApJ, 677, 704

Li, Y.-P., & Gan, W.-Q. 2011, Chinese Astronomy and Astrophysics, 35, 397

Li, Y. P., Gan, W. Q., & Feng, L. 2012, ApJ, 747, 133

Lotka, A. 1926, J. Wash. Acad. Sci., 16, 317

Newman, M. 2005, Contemporary Physics, 46, 323

Orwig, L. E., Frost, K. J., & Dennis, B. R. 1980, Sol. Phys., 65, 25

Parnell, C. E., & Jupp, P. E. 2000, ApJ, 529, 554

Press, W. H., Teukolsky, S. A., Vetterling, W. T., & Flannery, B. P. 1992, Numerical Recipes in C: The Art of Scientific Computing (2nd ed.; Cambridge: Cambridge Univ. Press)

Roberts, D. C., & Turcotte, D. L. 1998, Fractals, 6, 351

Schwartz, R. A., Dennis, B. R., Fishman, G. J., et al. 1992, in NASA Conference Publication, 3137, eds. C. R. Shrader, N. Gehrels, & B. Dennis, 457

Shimizu, T. 1995, PASJ, 47, 251

Song, Q., Huang, G., & Tan, B. 2012, ApJ, 750, 160

Su, Y., Gan, W. Q., & Li, Y. P. 2006, Sol. Phys., 238, 61

Veronig, A., Temmer, M., Hanslmeier, A., Otruba, W., & Messerotti, M. 2002, A&A, 382, 1070

Willis, J. C., & Yule, G. U. 1922, Nature, 109, 177

Zipf, G. K. 1949, Human Behaviour and the Principle of Least Effort (Cambridge, MA: Addison-Wesley), 11, 2008